The IET

Engineering the future

Electronics Letters

Volume 42 Number 18 31st August 2006
ISSN 0013-5194

Contents

pages 1011–1068

31st August 2006 Vol. 42 No. 18

the QD VCSEL are at 1 and 0.6 mA. The time delays are 36 and 27 ps for −12 and −10 dBm, respectively, when the bias current is at 1 mA. In addition, the time delays against bias currents of the QD VCSEL and the optical power of probe signal are shown in Fig. 4*b*. We observe that the time delay increases as the signal power decreases.

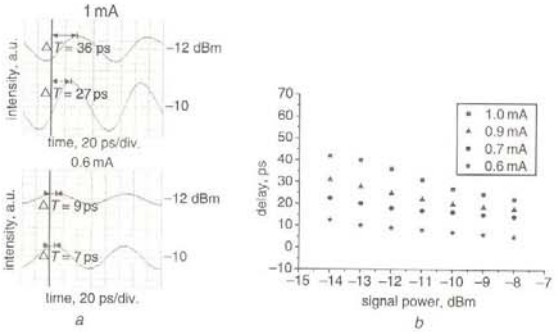

Fig. 4 *Waveform at different powers of probe signals; time delays against bias currents of QD VCSEL and optical power of probe signal*

a Waveform at different powers of probe signals
b Time delays against bias currents of QD VCSEL and optical power of probe signal

Conclusion: We have experimentally demonstrated tunable optical group delay in a 1.3 μm QD VCSEL at room temperature for the first time. The monolithic QD VCSEL based on GaAs substrate is the fully doped structure. Tunable delays of 42 ps for 10 GHz are achieved by varying the bias current.

Acknowledgments: The authors thank S.-L. Chuang (Department of Electrical and Computer Engineering, University of Illinois at Urbana-Champaign) for useful discussions and A.R. Kovsh (NL Nanosemiconductor GmbH) for his assistance and cooperation in epitaxial growth. This work is supported by the National Science Council, Republic of China, under contract NSC 94-2752-E-009-007-PAE.

26 April 2006
Electronics Letters online no: 20061316
doi: 10.1049/el:20061316

P.C. Peng, C.T. Lin, H.C. Kuo, W.K. Tsai, S. Chi, and S.C. Wang (*Department of Photonics and Institute of Electro-Optical Engineering, National Chiao Tung University, 1001 Ta Hsueh Road, Hsinchu, Taiwan 300, Republic of China*)

E-mail: pcpeng@mail.nctu.edu.tw; hckuo@faculty.nctu.edu.tw

G. Lin, H.P. Yang, K.F. Lin and J.Y. Chi (*Opto-Electronics and System Laboratory, Industrial Technology Research Institute, Hsinchu, Taiwan 300, Republic of China*)

References

1 Yang, H.P., Chang, Y.H., Lai, F.I., Yu, H.C., Hsu, Y.J., Lin, G., Hsiao, R.S., Kuo, H.C., Wang, S.C., and Chi, J.Y.: 'Singlemode InAs quantum dot photonic crystal VCSELs', *Electron. Lett.*, 2005, **41**, (20), pp. 1130–1132
2 Chang, Y.H., Lin, G., Kuo, H.C., Chi, J.Y., and Wang, S.C.: 'Singlemode monolithically quantum-dot vertical-cavity surface-emitting laser in 1.3 μm with side-mode suppression ratio > 30 dB'. IEEE Lasers and Electro-Optics Society 2005 Annual Mtg (LEOS 2005), Paper No. TuAA4, pp. 400–401, 2005
3 Minin, S., Fisher, M.R., and Chuang, S.L.: 'Current-controlled group delay using a semiconductor Fabry-Perot amplifier', *Appl. Phys. Lett.*, 2004, **84**, pp. 3238–3240
4 Zhao, X., Palinginis, P., Pesala, B., Chang-Hasnain, C.J., and Hemmer, P.: 'Tunable ultraslow light in vertical-cavity surface-emitting laser amplifier', *Opt. Express*, 2005, **13**, pp. 7899–7904
5 Yu, H.C., Chang, S.J., Su, Y.K., Sung, C.P., Lin, Y.W., Yang, H.P., Huang, C.Y., and Wang, J.M.: 'A simple method for fabrication of high speed vertical cavity surface emitting lasers', *Mater. Sci. Eng. B*, 2004, **106**, pp. 101–104

800–5000 MHz ultra-wideband CPW balun

J.-S. Lim, U.-H. Park, Y.-C. Jeong, K.-S. Choi, D. Ahn, S. Oh and J.-J. Koo

An ultra-wideband coplanar waveguide (CPW) balun for operation over 800–5000 MHz using a commonly used hybrid microwave substrate is proposed. The CPW balun consists of a multistage Wilkinson structure, an 'X'-shaped phase inverting structure, bottom-bridges and via-holes. The proposed balun does not need any additional circuit area for the generation of out-of-phase characteristics, so its size is exactly that of the basis Wilkinson divider.

Introduction: A balun having Wilkinson structure (hereinafter 'Wilkinson balun') is one of the widely used high frequency components since its basic structure looks like a Wilkinson divider. The previous Wilkinson baluns require an additional circuit area compared to the basic Wilkinson divider to realise the out-of-phase inverting section such as Lange couplers with open/short terminations or couplers having a two-wire coaxial cable [1–3]. In this Letter, a new CPW Wilkinson balun having compact size but ultra-wide frequency band is proposed and discussed.

Multi-stage ultra-wideband Wilkinson divider: To broaden the bandwidth of Wilkinson dividers, it is required to increase the number of stages [4, 5], e.g. to obtain the frequency ratio of 10 ($=F_{highest}/F_{lowest}$) a seven-stage Wilkinson divider should be realised ideally. However, the practically obtainable ratio must be less than 10 since CPW circuits and discontinuity elements such as bend and Tee-junction need many air-bridges which are the cause of performance degradation and band limitation.

Proposed ultra-wideband CPW balun: To make the out-of-phase section of the CPW balun, the 'X'-shaped crossing structure is adopted between signal and ground lines [6–9]. Fig. 1 shows the seven-stage ultra-wideband CPW Wilkinson divider ('basis divider') and balun, and the magnified phase inverting structure. Because the phase inverting section has ideally wideband characteristics, the ultra-wide operating band of the Wilkinson divider is directly converted to the wideband balun performances.

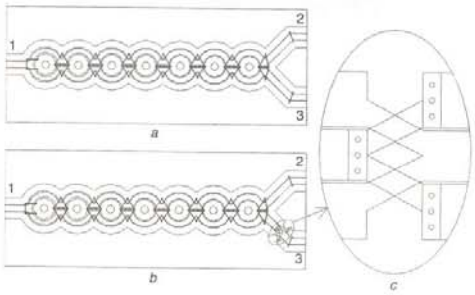

Fig. 1 *Ultra-wideband CPW divider and balun*

a Divider
b Balun
c CPW phase inverting structure

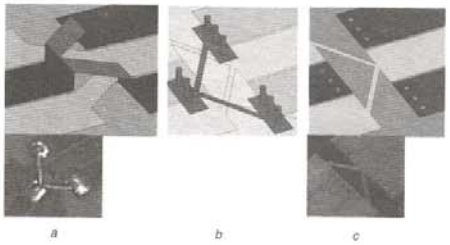

Fig. 2 *Layout and photos of bridge structures for phase inversion*

a Air-bridge
b 3-d view of bottom-bridge and via-holes
c Top plate layout of bottom-bridge connection

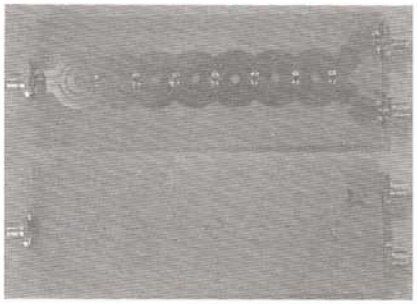

Fig. 3 *Fabricated CPW balun*

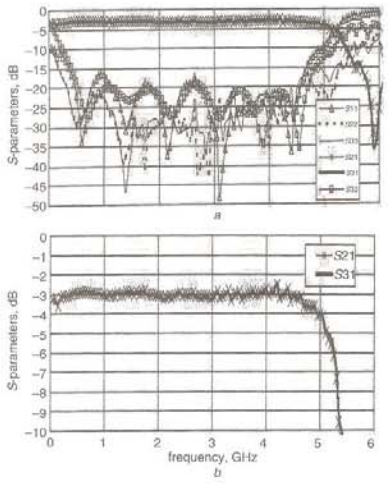

Fig. 4 *Measured S-parameters of wideband divider*

a *S*-parameters
b Comparison between *S*21 and *S*31

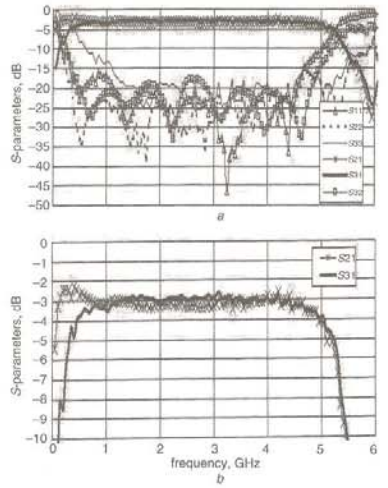

Fig. 5 *Measured S-parameters of wideband balun*

a *S*-parameters
b Comparison between *S*21 and *S*31

However, when it is realised practically using conventional hybrid microwave integrated circuits (HMICs) technology, much troublesome manual work is required because of the many air-bridges. To avoid this cumbersome manual operation, the bottom-bridge connection having via-holes can be selected as shown in Figs. 2*b* and *c*. Of course, it is noted that bottom-bridges having via-holes are the cause of performance degradation and band limitation from ideal characteristics in HMIC technology. However, the situation becomes worse for conventional air-bridges by manual working as shown in Fig. 2*a*.

Fabrication and measurement: The proposed CPW balun has been designed and fabricated using a microwave substrate having dielectric constant of 2.2 and thickness of 31 mils. Fig. 3 shows the top and bottom planes of the realised CPW balun. Even though the Wilkinson divider is not shown here, its size is exactly the same as in Fig. 3.

Figs. 4 and 5 are the measured *S*-parameters of the basis Wilkinson divider and the proposed CPW balun. Even their bandwidths have not extended up to the intended 6 GHz owing to so many parasitic elements such as bottom-bridges and via-holes the frequency band covers from 800 to 5000 MHz. Furthermore, it is important that the measured bandwidth and *S*-parameters of the balun in Fig. 5 are very similar to those of the basis divider in Fig. 4. So, the proposed balun preserves the ultra-broad bandwidth at no cost in size and performance, once the basis Wilkinson divider has wideband characteristics. Fig. 6 shows that the measured out-of-phase characteristics of the fabricated balun are $(180 \pm 10)^\circ$ over 800 to 5000 MHz.

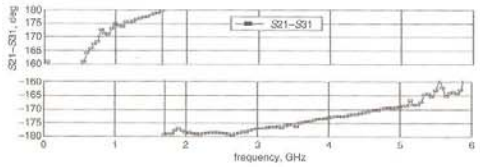

Fig. 6 *Measured out-of-characteristic of wideband balun*

Conclusion: A CPW balun from 800 to 5000 MHz is proposed and fabricated using a commonly used hybrid microwave substrate and MIC technology. The measured amplitude and phase unbalances at output ports are ± 0.45 dB and $\pm 10^\circ$, respectively, over 800–5000 MHz. It is expected that the bandwidth, *S*-parameters and phase performances can be substantially improved if air-bridges are realised by MMIC or multi-layer fabrication technologies.

Acknowledgments: This work has been financially supported by the Ministry of Education and Human Resources Development (MOE), the Ministry of Commerce, Industry and Energy (MOCIE), and the Ministry of Labor (MOLAB) through the fostering project of the Laboratory of Excellency.

23 May 2006
Electronics Letters online no: 20061448
doi: 10.1049/el:20061448

J.-S. Lim, K.-S. Choi, D. Ahn, S. Oh and J.-J. Koo (*Division of Information Technology Engineering, Soonchunhyang University, Asan, Chungnam, Republic of Korea*)

E-mail: jslim@sch.ac.kr

U.-H. Park (*Kangwon National University, Republic of Korea*)

Y.-C. Jeong (*Division of Electronics and Information Engineering, Chonbuk National University, Republic of Korea*)

References

1 Rogers, J., and Bhatia, R.: 'A 6 to 20 GHz planar balun using a Wilkinson divider and lange couplers'. IEEE MTT-S Dig., June 1991, pp. 865–868
2 Park, U.H., and Lim, J.S.: 'A 700- to 2500-MHz microstrip balun using a Willkinson divider and 3-dB quadrature couplers', *Microw. Opt. Technol. Lett.*, 2005, **47**, (4), pp. 333–335
3 Lim, J.S., Yang, H.S., Lee, Y.T., Kim, S., Seo, K.S., and Nam, S.: 'E-band Wilkinson balun using CPW MMIC technology', *Electron. Lett.*, 2004, **40**, (14), pp. 879–880
4 Young, L.: 'Tables for cascaded homogeneous quarter-wave transformers', *IRE Trans. Microw. Theory Tech*, 1959, **MTT-7**, (4), pp. 233–328
5 Cohn, S.B.: 'A class of broadband three-port TEM-mode hybrids', *IEEE Trans. Microw. Theory Tech.*, 1968, **MTT-16**, (2), pp. 110–116
6 Kao, C.W., and Chen, C.H.: 'Miniaturized uniplanar 180° hybrid-ring couplers with $0.8\lambda_g$ and $0.67\lambda_g$ circumferences'. APMC Dig., 2000, pp. 217–220

7 Lim, J.S., Kim, D.J., Jeong, Y.C., and Ahn, D.: 'A size-reduced CPW balun using a "X"-crossing structure'. EUMC Dig., 2005, Paris, France, pp. 521–524
8 Wang, T., and Wu, K.: 'Size-reduction and band-broadening design technique of uniplanar hybrid ring coupler using phase inverter for M(H)HIC's', *IEEE Trans. Microw. Theory Tech.*, 1999, **47**, (2), pp. 198–206
9 Murgulescu, M.H., Moisan, E., Leguad, P., Penard, E., and Zaquine, I.: 'New wideband $0.67\lambda_g$ circumferences 180° hybrid ring coupler', *Electron. Lett.*, 1994, **30**, (4), pp. 299–300

Coaxial probe in circular cylindrical cavity

J.H. Kim, H.J. Eom and M.Y. Park

Scattering from a conducting circular cylindrical cavity fed by a coaxial probe is studied. A fast convergent series solution is obtained by utilising the results of monopole radiation in parallel plates. Numerical results agree well with other existing results.

Introduction: Conducting circular cylindrical cavities fed by coaxial probes have been used for microwave heating applicators and permittivity sensors. Coaxial probes have been widely used as feeding structures in microwave devices and antennas. Electromagnetic scattering from a conducting circular cylindrical cavity fed by a coaxial probe is therefore an important canonical problem. Scattering from the cavity fed by a coaxial probe extending to the top surface of the cavity was studied in [1, 2]. Scattering from a cavity fed by an open-ended coaxial line was also studied in [3]. Scattering from a cavity fed by a coaxial probe of any arbitrary length is a practically useful, important problem but the problem has not been rigorously studied yet. This Letter analyses scattering from a cylindrical cavity fed by a coaxial probe of any arbitrary length situated at the centre of the cavity. The problems considered in [1–3] are special cases of the problem addressed in this Letter. It is possible to solve the boundary-value problem of a cylindrical cavity fed by a coaxial probe and this Letter presents its solution based on eigenfunction expansions in conjunction with mode matching, Fourier transform, and residue calculus. Since the geometry of a coaxial probe in a circular cylindrical cavity is similar to that of a monopole in parallel plates in [4], the problem of a coaxial probe in a circular cylindrical cavity can be solved by slightly modifying the existing results in [4]. Notations and formulations used in this Letter closely follow those in [4]. A summary of theoretical formulation and numerical results is given in the following Section.

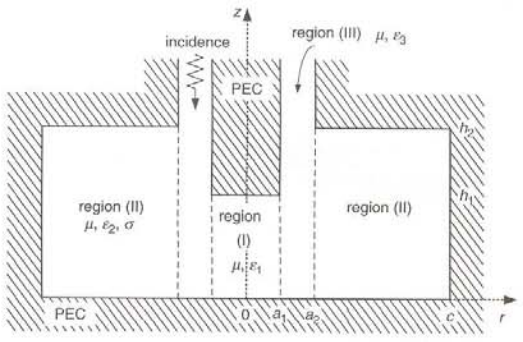

Fig. 1 *Geometry of circular cylindrical cavity excited by coaxial probe*
c and h_2 are radius and height of cavity, respectively. Coaxial probe has radius a_1 and length $(h_2 - h_1)$

Field analysis and computation: Consider a coaxial probe in a conducting circular cylindrical cavity, as shown in Fig. 1. The coaxial probe of arbitrary length $(h_2 - h_1)$ situated along the z-direction at $r = 0$ excites the cylindrical cavity. Owing to symmetry in the azimuthal ϕ direction, field variation is independent of ϕ. A time convention exp $(-i\omega t)$ is suppressed throughout. In region (III) $(a_1 < r < a_2, 0 < z < \infty)$, the total field consists of the incident, reflected, and scattered components. The expressions of the incident, reflected, and scattered fields are available in [4]. In region (I) $(0 < r < a_1, 0 < z < h_1)$ and region (II) $(a_2 < r < c, 0 < z < h_2)$, the scattered fields are represented as

$$E_z^I(r,z) = \frac{i}{\omega\varepsilon_1}\sum_{m=0}^{\infty} p_m \xi_{1m}\cos(h_{1m}z)J_0(\xi_{1m}r) \tag{1}$$

$$E_z^{II}(r,z) = \frac{i}{\omega\varepsilon_2}\sum_{m=0}^{\infty} p_m \xi_{2m}\cos(h_{2m}z)JQ_0(\xi_{2m}r) \tag{2}$$

where

$$h_{pm} = \frac{m\pi}{h_p}, \quad \xi_{pm} = \sqrt{k_p^2 - h_{pm}^2}$$

and

$$Q(\xi_{2m}r) = J_0(\xi_{2m}r)N_0(\xi_{2m}c) - N_0(\xi_{2m}r)J_0(\xi_{2m}c) \tag{3}$$

The expressions $J_0(\cdot)$ and $N_0(\cdot)$ are the 0th-order Bessel and Neumann functions, respectively. To determine the unknown modal coefficients p_m and q_m, the boundary conditions of E_z and H_ϕ field continuities must be enforced. The procedure of applying the boundary conditions is similar to that in [4], yielding

$$I_1 + p_n\frac{h_1}{2}J_1(\xi_{1n}a_1)\alpha_n = -\frac{2}{\eta}\frac{F_n^1(k_3)}{a_1} \tag{4}$$

$$I_2 - q_n\frac{h_2}{2}Q'(\xi_{2n}a_2)\alpha_n = -\frac{2}{\eta}\frac{F_n^2(k_3)}{a_2} \tag{5}$$

where $\alpha_0 = 2$, $\alpha_n = 1$ $(n = 1, 2, \ldots)$, $\eta = \sqrt{\mu/\varepsilon_3}$ and $Q'(\cdot) = dQ(\cdot)/d(\cdot)$. The expressions I_1 and I_2 are obtained by replacing $H_0^{(1)}(\xi_{2m}a_2)$ in [4, equations (11) and (13)] with $Q(\xi_{2m}a_2)$. The expressions $F_n^1(k_3)$ and $F_n^2(k_3)$ are available in [4]. Equations (4) and (5) constitute a set of simultaneous equations for the unknown modal coefficients p_m and q_m. The reflected plus scattered TEM field at $z = \infty$ in region (III) is also given by the series in [4, equations (17)–(19)] with $H_0^{(1)}(\xi_{2m}a_2)$ replaced by $Q(\xi_{2m}a_2)$. Computations are performed to check the accuracy of our series solution. Fig. 2 shows the phase of the reflection coefficient against frequency for the three different probe lengths $(h_2 - h_1)$. The comparison between our results when $h_2 - h_1 = 150$ mm and the unsheathed case of [2] indicates good agreement. Table 1 shows the convergence behaviour of $|p_m|$ and $|q_m|$ against the mode numbers m for the cases given in Fig. 2. The number of modes m used in our computation is five to achieve convergence to better than 1% error. Figs. 3 and 4 show the behaviour of the reflection coefficient when region (II) of the cavity is filled with a lossy dielectric material. Comparison between the Ansoft HFSS results and ours shows good agreement. The magnitude and phase of the reflection coefficient becomes oscillatory as frequency increases. Our theoretical analysis based on eigenfunction expansions yields very simple yet rigorous expressions, which are not only efficient for computation but also useful for practical applications.

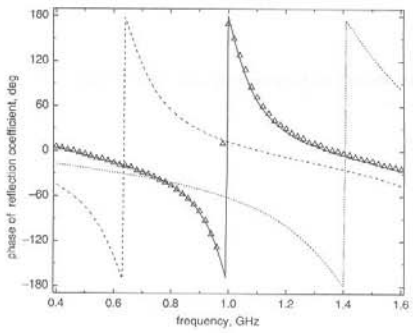

Fig. 2 *Phase of reflection coefficient against frequency for different probe length $(h_2 - h_1)$*
$a_1 = 1.525$ mm, $a_2 = 3.5$ mm, $c = 41$ mm, $h_2 = 150$ mm, $\varepsilon_{r1} = \varepsilon_{r2} = \varepsilon_{r3} = 1$, $\sigma = 0$ s/m
—— $h_2 - h_1 = 150$ mm
- - - - $h_2 - h_1 = 110$ mm
..... $h_2 - h_1 = 45$ mm
Δ Keam and Williamson [2]